Journal of Chromatography B, 1033–1034 (2016) 342–352

Contents lists available at ScienceDirect

Journal of Chromatography B

journal homepage: www.elsevier.com/locate/chromb

Applying mini-bore HPAEC-MS/MS for the characterization and quantification of Fc *N*-glycans from heterogeneously glycosylated IgGs

Maria Maier[a], Dietmar Reusch[a], Cees Bruggink[b], Patrick Bulau[a], Manfred Wuhrer[b], Michael Mølhøj[c,*]

[a] *Pharma Technical Development Penzberg, Roche Diagnostics GmbH, Nonnenwald 2, D-82377 Penzberg, Germany*
[b] *Center for Proteomics and Metabolomics, Leiden University Medical Center, PO Box 9600, 2300 RC Leiden, The Netherlands*
[c] *Roche Pharma Research and Early Development, Large Molecule Research, Roche Innovation Center Munich, Roche Diagnostics GmbH, Nonnenwald 2, D-82377 Penzberg, Germany*

ARTICLE INFO

Article history:
Received 27 April 2016
Received in revised form 12 July 2016
Accepted 2 August 2016
Available online 9 August 2016

Keywords:
HPAEC-MS/MS
Mass spectrometry
Pulsed amperometric detection
N-Glycan
IgG
Oligosaccharides
Sialyltransferase

ABSTRACT

High-performance anion-exchange chromatography (HPAEC) coupled to pulsed amperometric detection (PAD) is a highly sensitive method for the analysis of oligosaccharides without the need for prior derivatization. However, the method suffers from the lack of chemical information with peak assignments based on the retention times of authentic standards or known peaks of reference materials. Here we applied HPAEC coupled on-line with electrospray ion trap mass spectrometry (HPAEC-MS) using a prototype mini-bore (1 mm I.D.) CarboPac PA200 column and challenged the analytical separation based method for the structural assignment of heterogeneous mixtures of *N*-glycans derived from immunoglobulin G from human plasma, glyco-engineered CHO cells, and Sp2/0 mouse myeloma cells. Compared to an analytical scale 3 mm I.D. column, the mini-bore column demonstrated a superior performance with up to 8-fold improved limit of detection for specific *N*-glycans determined by PAD. Quantitative evaluation by extracted ion current chromatograms revealed detection limits in the 50–100 femtomole range using ion trap MS operated in positive ionization mode. In our hands HPAEC-MS/MS allowed the detection and quantification of even low abundant glycan species including biantennary complex-type, high mannose, hybrid and hybrid bisected structures. In comparison to the detection of *N*-glycans as lithiated or sodiated adducts, we obtained a 65-fold improved signal-to-noise ratio with protonated ions only. Relative quantitative evaluation by single ion current chromatograms was successfully applied and demonstrated an excellent performance with respect to selectivity in the relative quantification of heterogeneous samples of *N*-glycans compared to HPAEC-PAD and HILIC-UPLC of 2-AB labelled *N*-glycans.

1. Introduction

The distribution and type of *N*-linked glycans may be critical in the pharmacology of monoclonal antibodies (mAbs), one of the most important classes of biologicals, potentially affecting parameters like protein–protein interactions, immunogenicity, pharmaco-kinetics and −dynamics [1]. For these reasons the necessary product quality monitoring of therapeutic proteins requires high resolving and sensitive analytical tools for the characterization of their glycosylation [2]. High-performance anion-exchange chromatography (HPAEC) allows a powerful separation of carbohydrates as their hydroxyl groups are in part deprotonated to oxyanions at high pH (>13.5). Due to subtle differences in the pK_a values of the different hydroxyl groups, the oxyanions of carbohydrates generated under highly alkaline conditions interact differently with the positively charged stationary phase and facilitate their separation by anion-exchange mechanisms. This column interaction is influenced by differences in size, linkage isomerism, composition, charge, and branching of the carbohydrates [3–6]. Coupling of HPAEC to sensitive pulsed amperometric detection (PAD) including gold electrode catalyzed anodic electro-oxidation has been successfully applied to a wide range of carbohydrates and oligosaccharides [4,6–9] with sensitivities down to picomole levels [4,5,10]. Rohrer [11] and Behan and Smith [6] summarized the influence on the retention time of the structure of *N*-linked oligosaccharides, e.g. the presence of sialic acids (α2,3- or α2,6-linked), bisected GlcNAc, and number of β1,4-Gal residues linked to GlcNAc. PAD detection does not directly provide any structural

* Corresponding author.
E-mail address: michael.molhoj@roche.com (M. Mølhøj).

http://dx.doi.org/10.1016/j.jchromb.2016.08.001

information needed for correct assignment of structurally complex *N*-glycans in a chromatogram. Due to the lack of several authentic standards (e.g. hybrid bisected structures), correct structure assignment by HPAEC coupled with mass spectrometry will be very useful.

The analysis of oligo- and polysaccharides by HPAEC coupled to on-line desalting of the high salt concentrated eluent and mass spectrometry has been described [12–19]. Nevertheless, the application of HPAEC with on-line MS has been partly hampered by the lack of commercially available small-bore LC columns with their improved influence on gain in sensitivity, peak broadening, and increased compatibility with low flow detection methods like MS. Miniaturized desalting units to suppress the ions of the alkaline mobile-phase as reported by Wouters et al. [20] have the potential to further optimize the in-line coupling with mass spectrometric detection.

Here we report the application of 1 mm I.D. size HPAEC using a prototype CarboPac PA200 column coupled to PAD detection or on-line ion trap mass spectrometry for the structural assignment and quantification of *N*-linked oligosaccharides. To challenge the method, heterogeneous *N*-glycans from various sources of IgGs were analyzed including from human plasma derived IgG, a CHO produced monoclonal antibody glyco-engineered for non-fucosylation, a Sp2/0 mouse myeloma cell line produced monoclonal antibody and the latter antibody additionally α2,6-sialylated with Neu5Ac. The aim of this study was to couple HPAEC and MS to efficiently characterize heterogeneous *N*-glycan mixtures and to extend the range of application with respect to sensitivity by coupling mini-bore HPAEC with on-line MS. Structural assignments based on molecular mass determination and fragment ion formations were supported by digests with exo-glycosidases and spiking with available *N*-glycans standards.

2. Material and methods

2.1. Reagents, standards and enzymes

Analytical reagent grade sodium acetate anhydrous (BioUltra) and sodium hydroxide (50%) were obtained from Sigma Aldrich Chemie (Steinheim, Germany). $NaH_2PO_4 \cdot H_20$, NaCl and LiCl were obtained from Merck (Darmstadt, Germany). Acetonitrile was purchased from J.T. Baker (Deventer, The Netherlands). All solutions were prepared with water from a Milli-Q System (Millipore, Billerica, MA). Helium gas (99.999%-mol) was obtained from Linde (Munich, Germany). The *N*-glycan standards FA2 (Oxford notation), A2, FA2B, and FA2G2NeuAc1 for LOD determinations were obtained from Prozyme (Hayward, CA). The *N*-glycan standards FA2G1NeuAc1(3) (3 denoted *α2,3-linked* Neu5Ac), FA2G2NeuAc1(3), FA2G1NeuAc1(6) (6 denoted *α2,6-linked* Neu5Ac), FA2G2NeuAc1(6), FA2G2NeuAc2(6), and FA2G2Gal1 were obtained from TheraProteins (Barcarena, Portugal). PNGase F, CMP-Neu5Ac, the *Arthrobacter ureafaciens* neuraminidase (EC 3.2.1.18) releasing α2,3/6/8-linked non-reducing terminal Neu5Ac and Neu5Gc, and the recombinant human β-galactoside α2,6-sialyltransferase 1 ST6Gal-I (EC 2.4.99.1) were obtained from Roche Diagnostics GmbH (Mannheim, Germany). The α-galactosidase from green coffee beans (EC 3.2.1.22) releasing non-reducing terminal α1,3/4/6-linked galactose from oligosaccharides, the *Streptococcus pneumonia* β1,4-galactosidase (EC 3.2.1.23) hydrolyzing non-reducing terminal β1,4-galactose, the recombinant *S. pneumonia* β-*N*-acetylglucosaminidase (EC 3.2.1.30) hydrolyzing β1,4-GlcNAc linked to mannose (except for bisecting GlcNAc), and the recombinant *S. pneumoniae* Sialidase S (EC 3.2.1.18) releasing α2,3-linked non-reducing terminal Neu5Ac and Neu5Gc were obtained from Prozyme (Hayward, CA).

2.2. Antibodies

The monoclonal antibodies of the IgG1 type denoted mAb1, mAb2 and mAb4 expressed in Chinese hamster ovary (CHO) cells, the mAb3 produced in Sp2/0 mouse myeloma cells, and the purified IgG from human plasma (h-IgG, 99%), were obtained from Roche Diagnostics (Penzberg, Germany). All mAbs contain *N*-glycans only in their Fc domains.

2.3. Preparation of N-glycans

400 μg proteins was buffer exchanged by gravity flow on a NAP-5 column (GE Healthcare, Freiburg, Germany), equilibrated with 10 mL and eluted with 450 μL 10 mM NaH_2PO_4, pH 7.2. The eluted protein was concentrated to 50 μL on a Vivaspin 500 concentrator (10 kDa cut off; Sartorius, Göttingen, Germany) by centrifugation. The *N*-glycans were released by adding 2 U of PNGase F (37 °C for 18 h) and isolated by passing over a Vivaspin 500 concentrator followed by washing the concentrator with 2 × 30 μL water. To the total flow-through and washes, water was added to 140 μL. *N*-glycans were digested with 20 mU neuraminidase, 0.5 U α-galactosidase, 20 mU β1,4-galactosidase, or 6 U β-*N*-acetylglucosaminidase by adding the exoglycosidases to the PNGase F digest. α2,3-linked sialic acids were removed by incubating the PNGase F-released *N*-glycans with 120 mU Sialidase S at 37 °C for 2 h.

2.4. α2,6-Sialylation of mAb3

The α2,6-sialylation of the Sp2/0 derived mAb3 was performed by incubating 800 μg antibody with 400 μg CMP-Neu5Ac and 80 μg α2,6-sialyltransferase (ST6Gal-I) in water (140 μL) at 37 °C for 4 h. Finally, the sialylated mAb3 was purified using a 400 μL ProSep®-vA High Capacity column (Millipore) equilibrated with ten column volume equilibration buffer (25 mM Tris, 25 mM NaCl, 5 mM EDTA pH 7.1) to remove excess CMP-Neu5Ac. The column was washed first with four column volume equilibration buffer, then two column volume 1 M Tris pH 7.2, and finally with four column volume equilibration buffer. The sialylated mAb3 was eluted with two column volume 25 mM sodium citrate pH 2.8 and the pH adjusted to 7.0 with 1 M Tris pH 9.0.

2.5. High-performance anion-exchange chromatography (HPAEC)

The *N*-glycan analysis was performed using a ICS2500 chromatography system from Thermo Fischer Scientific (Sunnyvale, CA) controlled by the Chromeleon software (Version 6.8 SP2, Thermo Fischer Scientific) and consisting of an AS50 autosampler with sample cooling, a GS50 low pressure quaternary gradient pump with an online degasser, an ED50A electrochemical detector and a flow-through cell equipped with a disposable gold electrode and a pH reference electrode. 9 μL injections were performed using a 10 μL injection loop. The columns used included a CarboPac PA200 (3 × 250 mm) and a prototype mini-bore size CarboPac PA200 (1 × 250 mm) obtained from Thermo Fischer Scientific (Idstein, Germany). Both CarboPac PA200 columns are packed with 5.5 μm polyethylvinylbenzene-divinylbenzene copolymer particles. These copolymer particles have at the surface electrostatically bound microbeads of 46 nm functionalized with strong anion exchange groups. The columns, preceded by a Borate Trap column (4 mm × 50 mm; Thermo Fischer Scientific, Idstein, Germany) between the pump and the injection valve, were equilibrated with initial conditions of the separation gradient. Using the 1 mm column, all experiments were executed at ambient temperature using a flow rate of 0.6 mL min^{-1} prior to a pre-column split with a column flow rate of 50 μL min^{-1}. The 3 mm column was used with

a column flow rate of 0.5 mL min^{-1}. Eluents were prepared by degassing with helium and kept saturated with helium gas to minimize adsorption of CO_2. Elution was achieved with linear gradients of eluent A (50 mM NaOH) and eluent B (50 mM NaOH, 200 mM NaOAc). mAb1: isocratic 0% B (0–2 min), linear acetate gradients to 2% B (2–8 min), 3% B (8–15 min), 7% B (15–25 min), 50% B (25–55 min), 100% B (55–56 min), isocratic 100% B (56–61 min), gradient to 0% B to convert the column into the hydroxide form (61–62 min), and isocratic equilibration of the column with 0% B (62–70 min). MAb2 and h-IgG: isocratic 0% B (0–2 min), linear acetate gradients to 1% B (2–5 min), 3% B (5–25 min), 20% B (25–55 min), 50% B (55–70 min),100% B (70–70.1 min), isocratic 100% B (70.1–75 min), gradient to 0% B (75–75.1 min), and equilibration with 0% B (75.1–80 min). mAb3 and mAb4: isocratic 0% B (0–2 min), linear acetate gradient to 1% B (2–5 min), 3% B (5–25 min), 20% B (25–55 min), 70% B (55–90 min), 100% B (90–90.1 min), isocratic 100% B (90.1–95 min), gradient to 0% B (95–95.1 min), and equilibration with 0% B (95.1–100 min). The samples were injected at 0 min and all separations were performed at room temperature.

2.6. Pre-column eluent flow splitting

To obtain a flow rate of 50 μL min^{-1}, a flow splitter was inserted between the gradient pump and the autosampler. The eluent was split (ratio 1:11) via a TEE (model P-727, Upchurch Scientific, Oak Harbor, WA) connected to the analytical column and to waste.

2.7. Pulsed amperometric detection

The amperometric detector was coupled to the outlet of the analytical column, and pulsed amperometric detection obtained using the following pulse potentials and time settings: E_1 = 0.1 V (t_d: 0.00-0.20 s, t_1: 0.20-0.40 s), E_2 = −2.0 V (t_2: 0.41–0.42 s), E_3 = 0.6 V (t_3: 0.43 s), E_4 = −0.1 V (t_4: 0.44–0.50 s). Quantitative evaluation was performed by integration of the PAD chromatograms using the Chromeleon software.

2.8. Desalting of the HPAEC effluent

The HPAEC effluents contained relatively high concentrations of non-volatile species and were made compatible with the ESI interface using a prototype 1 mm online carbohydrate membrane desalter (CMD 300, Thermo Fischer Scientific, Sunnyvale, CA) [21]. For continues regeneration the desalter was connected to a AXP-MS Auxiliary Pump (Thermo Fischer Scientific) at a flow rate of 150 μL min^{-1}. Water was used as regeneration solution. The CMD 300 contains membranes functionalized with strong cation exchange groups and exchanges sodium ions for hydronium ions. In this set-up, hydronium ions neutralize hydroxide to water and acetate is converted to acetic acid. Sodium ions are removed by diffusion into the cathode compartment.

2.9. Ion trap mass spectrometry

Electrospray ionization mass spectrometry (ESI–MS) and ESI–MS/MS was performed in the positive ion mode using a HCT Ultra PTM Discovery System ion trap mass spectrometer from Bruker Daltonics (Bremen, Germany). Make-up solutions were pumped into the eluent flow via a TEE (model P-727, Upchurch Scientific) and a Harvard syringe pump (model PHD 2000, Harvard Apparatus, Holliston, MA) equipped with a Hamilton 10 mL syringe at a flow rate of 15 μL min^{-1}, and the flow directed to the ESI interface of the mass spectrometer. The ESI–MS was operated using the following settings: dry gas temperature 300 °C, nebulizer 10 psi, dry gas 5 L min^{-1}, capillary voltage 4 kV, target mass 800 m/z, full scan range 500–1500 m/z, rolling averages with five spectra. Helium was used as collision gas. Noise reduction and spike removal was performed using MassMap software (MassMap, Wolfratshausen, Germany). MS/MS was performed in automatic mode using ramped CID voltage (SmartFrag, 30–200% fragmentation amplitude). The instrument was calibrated using TuneMix (Bruker Daltonics). MS and MS/MS spectra were evaluated using Data Analysis software (Bruker Daltonics). Carbohydrate structure determinations were performed with assistance from GlycoWorkbench [22].

2.10. Quantitative single ion current evaluation

Relative quantification of *N*-glycans by mass spectrometry was performed by automatic baseline integration of specific ion current (SIC) chromatograms on the basis of charge state 2+ and isotopes 0,1 and 2 using GRAMS AI software (Thermo Fisher Scientific, Dreieich, Germany).

3. Results and discussion

3.1. Ionization mode and test of make-up solutions

HPAEC-MS has previously been performed with on-line addition of a make-up solution containing either LiCl or NaCl following the on-line desalting [15,23] for improved ionization and to obtain informative spectra including not only B- and Y-type ions but also C and Z ions and cross-ring cleavages of the eluting oligosaccharides (nomenclature proposed by Domon and Costello [24]). In positive ionization mode the carbohydrates are then detected as lithiated or sodiated adducts ($[M+Li]^+$, $[M+Na]^+$, $[M+2Li]^{2+}$, $[M+2Na]^{2+}$). To test the ionization with alkali metals, we tested the influence and the composition of make-up solutions consisting of 1 mM NaCl in 50% (v/v) acetonitrile, 1 mM LiCl in 50% (v/v) acetonitrile, and 50% (v/v) acetonitrile. As the sodium acetate containing HPAEC eluent, after passing the desalter converted into acetic acid, might be sufficient to facilitate ionization and protonated ions, we speculated whether the make-up could possibly be omitted without further peak dilution. Total ion current chromatograms obtained in positive ion mode of about 300 pmol of *N*-glycans from mAb1, demonstrated signal-to-noise ratios (ratio of the signal peak height to 5 times the standard deviation of the noise) for FA2 (S/N_{FA2}) of 17, 47 (Fig. 1A), 256, and 3049 (Fig. 1B), for the make-up solutions; 1 mM NaCl in 50% (v/v) acetonitrile, 1 mM LiCl in 50% (v/v) acetonitrile, 50% (v/v) acetonitrile, and without the use of a make-up solution, respectively, demonstrating a considerably higher sensitivity without the use of a make-up. Without make-up solution, we detected proton adducts and about 1% sodium adducts. The level of in-source fragmentation (determined by comparing signal intensities of FA2 versus fragments FA1 and A2, charge states 2^+) was determined to be 15% using 1 mM LiCl in 50% acetonitrile compared to 3% without a make-up solution or 50% acetonitrile. Without make-up and further dilution of the eluting glycan structures, the MS/MS spectra allowed the identification of a total of 10 mAb1 derived *N*-glycans (FA1, A1, FA1G1, FA2, M5, A2, FA2G1, FA2G2, FA2G1, FA2G1NeuAc1, FA2G2NeuAc1; Fig. 1C), whereas with 1 mM LiCl/50% acetonitrile, only the most abundant *N*-glycans (FA2, FA2G1 and FA2G2) could be detected. As expected we detected fucose-rearrangements [25] only upon tandem mass spectrometry of the protonated precursor ions.

In negative ionization mode, we tested the following make-up solutions in 50% methanol (v/v): 100 mM NH_4OH, 100 mM NH_4OH/100 mM NH_4NO_3, 100 mM NH_4NO_3, and 200 mM NH_4NO_3 based on the study by Harvey [26], who demonstrated that nitrate adducts of the type $[M+NO_3]^-$ form stable complexes with *N*-glycans. With NH_4OH we detected *N*-glycans as $[M-H]^-$ ions and

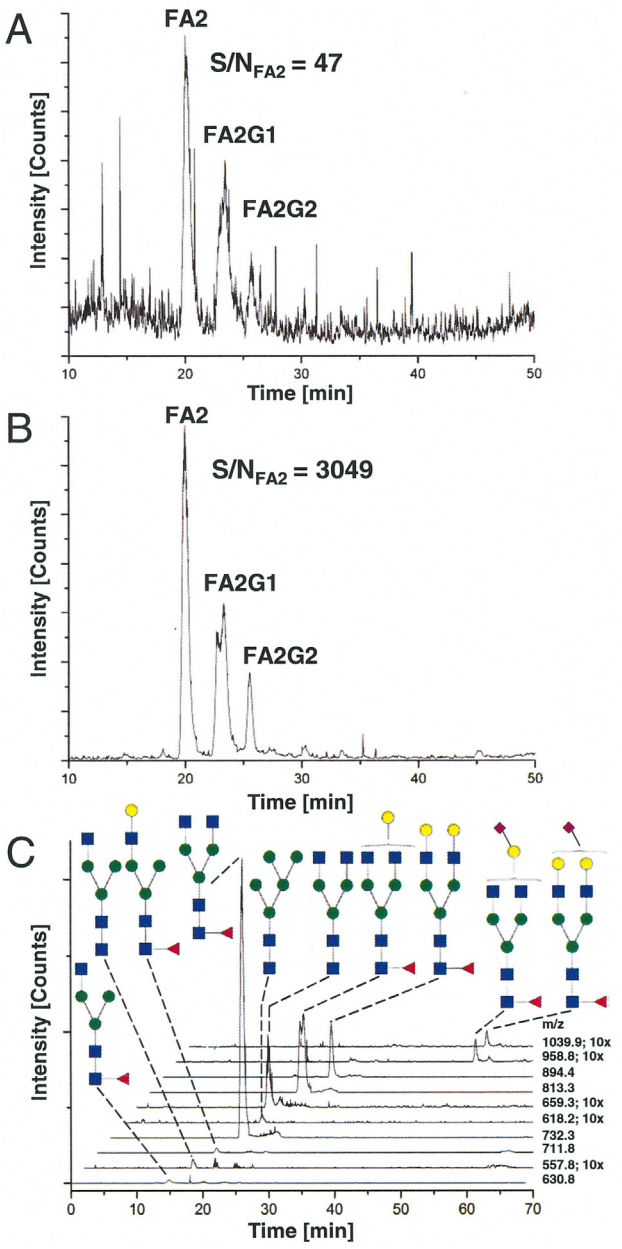

Fig. 1. Total ion current chromatograms from positive ion mode HPAEC-MS of PNGase F-released *N*-glycans from mAb1 with (A) a make-up solution of 1 mM LiCl in 50% acetonitrile (v/v), and (B) without the use of a make-up solution. Signal-to-noise ratios for FA2 (S/N_{FA2}) are indicated. (C) Stacked extracted ion current chromatograms obtained without make-up solution for all double-protonated *N*-glycans $[M+2H]^{2+}$ detected from mAb1 (*m*/*z* values are listed). *N*-glycans are given according to the Consortium for Functional Glycomics notation; the Oxford glycan nomenclature was used for the abbreviations. Blue square (GlcNAc), red triangle (Fuc), green circle (Man), yellow circle (Gal), pink rhomb (Neu5Ac).

with NH_4OH/NH_4NO_3 and NH_4NO_3, $[M+NO_3]^-$ adducted species were detected. Using 300 pmol of *N*-glycans from mAb1, the signal-to-noise ratio for FA2 detected in negative ionization mode for the make-up solutions listed were determined to be between 19 and 61, demonstrating an at least 50-fold higher sensitivity in positive ionization mode without the use of a make-up solution (Fig. 1B). Unfortunately, with these make-up solutions the ESI capillary was plugged following each run and had to be cleaned. We speculate that precipitation of ammonium acetate caused this problem. As efficient ionization of the eluting *N*-glycans was only obtained from protonated precursor ions and since we did not obtain better signals with on-line addition of make-up solutions in neither positive nor negative ion mode, we decided to directly analyze all glycan structures as protonated ions in the positive mode. With CID MS/MS of the protonated ions, we generally observed cleavage of glycosidic linkages only.

3.2. Evaluation of the sensitivity and the limit of detection

The maximum concentration of an analyte at the peak apex is proportional to $N^{½}/D^2$, where N denotes the plate count and D the inner diameter of the column [27]. A reduction of the inner column diameter from 3 mm of the analytical scale mid-size CarboPac PA200 column to 1 mm of a mini-bore version should consequently offer a theoretical 9-fold sensitivity increase when maintaining separation performance. To evaluate the sensitivity of the PAD and the MS detectors, signals were evaluated by gradient elution of the *N*-glycan standards FA2, A2, FA2B, FA2NeuAc1 using at least five different levels of each oligosaccharide covering a calibration range of 100 fmol–60 pmol. For maximum sensitivity, the PAD detector was used with new working electrodes. The calibration curve fitting values and the determined limit of detection (LOD) for the 3 and 1 mm columns are reported in Table 1. Both the PAD and MS signals were linear over the ranges investigated with R^2 coefficients > 0.999. The LODs were calculated based on the slope and the standard deviation of the response estimated by five repeated injections of each analyte in the range of 400–600 fmol. Sensitivity and determination of the LOD of the MS was performed by integration of extracted ion current chromatograms of the double-protonated ions at *m*/*z* 732.3^{2+} (FA2), *m*/*z* 659.3^{2+} (A2), *m*/*z* 833.9^{2+} (FA2B), and *m*/*z* 1039.9^{2+} (FA2G2NeuAc1).

Comparing the calibration slopes of the PAD signals obtained with the 1 mm column with those obtained with the 3 mm column, the mini-bore column demonstrated the expected higher sensitivity with approximately 7-, 8-, 8-, and 10-fold for FA2, A2, FA2B, and FA2G2NeuAc1, respectively. The LODs improved approximately 2-, 6-, 8- and 5-fold for FA2, A2, FA2B, and FA2G2NeuAc1, respectively (Table 1). The LODs in the selected ion mode for protonated adducts of FA2, A2, FA2B, and FA2G2NeuAc1, were determined to be 47–105 fmol using the mini-bore column. The equivalent LODs obtained with PAD were determined to be 9–59 fmol (Table 1).

3.3. Gradient optimization

The mobile phases in HPAEC have a profound influence on the selectivity and speed of the separation with strong alkaline eluents ensuring strong column interaction. Lowering the concentration of NaOH from commonly used 100 mM in the eluents has been reported to improve the resolution of neutral *N*-glycans analyzed by HPAEC [28]. To ensure optimal chromatographic separation, we tested several concentrations of NaOH between 25 and 100 mM and for the elution of sialylated *N*-glycans various concentrations (up to 300 mM) of pushing agent NaOAc. Separation e.g. between A2 and M5 in the case of mAb1 (Fig. 1C) and reduced retention times of sialylated *N*-glycans could be obtained using linear gradients with 50 mM NaOH and eluent B containing additional 200 mM NaOAc. These eluents were therefore used throughout this study. For optimal analysis, a gradient separation was developed for each source of *N*-glycans. Extracted ion current chromatograms were used to monitor and optimize the separation. This resulted in chromatographic runs of between 70 and 100 min. (Figs. 1 C, 2, 3 and 5). The peak broadening at half height in the total ion current chromatograms (without make-up solution) was only 20% of the PAD peak width (FA2 only) caused by the arrangement of desalter and ESI interface of the MS.

Table 1
Calibration curve results and obtained limit of detection (LOD) using the 1 and 3 mm x 250 mm CarboPac PA200 columns.

Column Dimension:	CarboPac PA200 3 mm × 250 mm				CarboPac PA200 1 mm × 250 mm					
Detection Method:	Pulsed Amperometric Detection				Pulsed Amperometric Detection				Ion Trap (Extracted Ion Current)			
N-glycan Standard[c]	Slope (S)	Y Intercept	Corr. Coeff. (R^2)	LOD[a] [fmol]	Slope (S)	Y Intercept	Corr. Coeff. (R^2)	LOD[a] [fmol]	Slope (S)	Y Intercept	Corr. Coeff. (R^2)	LOD[a,b] [fmol]
FA2 (G0F), *m/z* 732.3	1×10^{-4}	+0.0291	0.9999	66	7×10^{-4}	+0.0587	0.9999	38	5.52	−119.5	0.9999	58
A2 (G0), *m/z* 659.3	0.8×10^{-4}	+0.0188	0.9999	289	6×10^{-4}	+0.0289	0.9999	50	3.36	−280.6	0.9999	105
FA2B (G0FB), *m/z* 833.9	0.9×10^{-4}	+0.0097	0.9999	73	7×10^{-4}	−0.1418	0.9999	9	2.35	+30.5	0.9999	83
FA2G2NeuAc1 (G2S1F), *m/z* 1039.9	1×10^{-4}	+0.1442	0.9994	297	10×10^{-4}	+0.1481	0.9999	59	7.94	+374.8	0.9999	47

[a] LOD = 3.3 × σ/S, where σ is the standard deviation of the peak area (n = 5) at 400–600 fmol.
[b] Determined using ion trap mass spectrometry and extracted ion current chromatograms of double-protonated ions.
[c] Abbreviations according to the Oxford glycan nomenclature (alternative naming in parentheses).

Fig. 2. HPAEC-PAD chromatograms and total ion current chromatograms from positive-mode HPAEC-MS (intensity attenuation: 10^{-3} ×) of PNGase F-released *N*-glycans from (A) a purified human IgG (h-IgG, 99%), and (B) an IgG1 from chinese hamster cells, glyco-engineered for non-fucosylation (mAb2). *N*-glycans are given according to the Consortium for Functional Glycomics notation. Blue square (GlcNAc), red triangle (Fuc), green circle (Man), yellow circle (Gal), pink rhomb (Neu5Ac). A spike peak is indicated by an asterisk.

3.4. *Analysis of various sources of IgG Fc* N-*glycans*

Following optimization of the chromatographic conditions, the PNGase F-released *N*-glycans from human plasma (h-IgG), mAb2 and mAb3 were subjected to both HPAEC-PAD and HPAEC-MS/MS analysis using the 1 mm CarboPac PA200 column. The peak patterns obtained with HPAEC-MS were similar to those obtained with HPAEC-PAD (Figs. 2, 3 and 5). The HPAEC-MS/MS analysis of the *N*-glycans released from h-IgG revealed in total 15 different structures (Fig. 2A). Besides common structures like FA2 (27 min), FA2G1 (32.5 min), FA2G2 (37 min) and monosialylated structures like FA2G1NeuAc1(6) (6 denoted *α2,6-linked* Neu5Ac) and FA2G2NeuAc1(6) (55–60 min), several bisected structures were detected like FA2 B (34.5 min), A2 B (36.0 min), FA2BG1 (37.5 min), A2BG1 (39.0 min) and FA2BG2 (40.0 min) (Fig. 2A). Also the hybrid bisected structures; FM5A1 B (41.0 min), M5A1 B (42.5 min), and M5A1G1 B (43.5 min) were detected (Fig. 2A). The MS/MS spectrum of M5A1G1 B (*m/z* 902.9) is shown in Fig. 6A. The hybrid bisected structure is underpinned by the $B_3Y_3\beta$ fragment (*m/z* 852.3; D-ion) and $B_3Y_3\beta$ − 221 fragment (*m/z* 631.0; D-ion − 221) revealing the constitution of the 1,6-arm to be three hexoses [29]. This is also supported by fragments $Y_3\alpha Y_3\beta$ (*m/z* 790.3), $B_3\alpha Y_3\beta Y_{3\gamma}$ (*m/z* 649.0) and $B_3\beta$ (*m/z* 528.2) reveal-

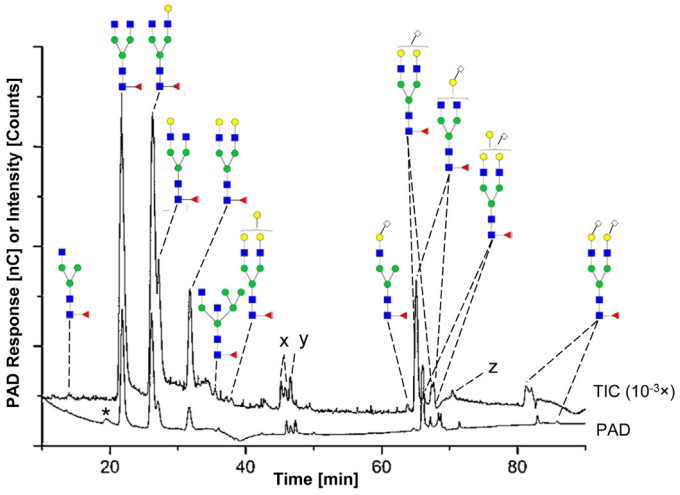

Fig. 3. HPAEC-PAD chromatograms and total ion current chromatograms from positive-mode HPAEC-MS (intensity attenuation: $10^{-3}\times$) of PNGase F-released *N*-glycans from mAb3 expressed in Sp2/0 mouse myeloma cells. The peaks x, y and z represent glycosylamines (*N*-glycan-1-amino-GlcNAc) of the *N*-glycans FA2G1NeuGc1(6) (two peaks), FA2G2NeuGc1(6) and FA2G2NeuGc2(6), respectively. *N*-glycans drawn based on the Consortium for Functional Glycomics notation. Blue square (GlcNAc), red triangle (Fuc), green circle (Man), yellow circle (Gal), white rhomb (Neu5Gc). A buffer component is indicated by an asterisk.

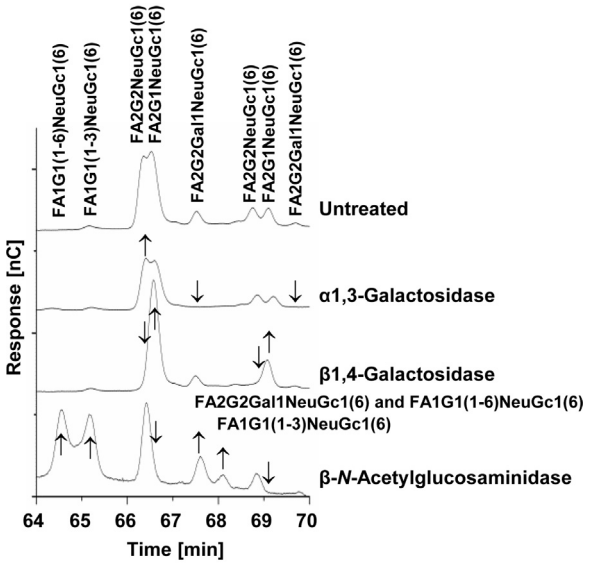

Fig. 4. The identity of the sialylated oligosaccharides of mAb3 eluting between 65 and 70 min (Fig. 3) was confirmed by HPAEC-MS and −PAD following digestions with α1,3- and β1,4-galactosidases and β-*N*-acetylglucosaminidase; arrows indicate the relative influence on the level of the eluting *N*-glycans.

ing the constitution of the 1,3-arm to be two hexoses and one *N*-acetylhexosamine, see also Table S1 in Supplementary materials. Unlike other serum glycoproteins with α2,3 sialic acid residues linked to penultimate galactose residues of *N*-glycans, human IgGs mainly contain *N*-glycans with α2,6-linked Neu5Ac [30,31]. Consequently, the Neu5Ac of the mono-sialylated FA2G1NeuAc1(6) and FA2G2NeuAc1(6) eluting between 55 and 60 min could only be removed with the *A. ureafaciens* neuraminidase releasing α2,3/6-linked sialic acids and not with the *S. pneumoniae* Sialidase S releasing α2,3-linked sialic acids (data not shown). Also, spiking of *N*-glycan standards FA2G1NeuAc1(6) (6 denoted *α2,6-linked* Neu5Ac), FA2G2NeuAc1(6), FA2G1NeuAc1(3) (3 denoted *α2,3-linked* Neu5Ac), FA2G2NeuAc1(3), confirmed the α2,6-linkage of the Neu5Ac structures of h-IgG (data not shown).

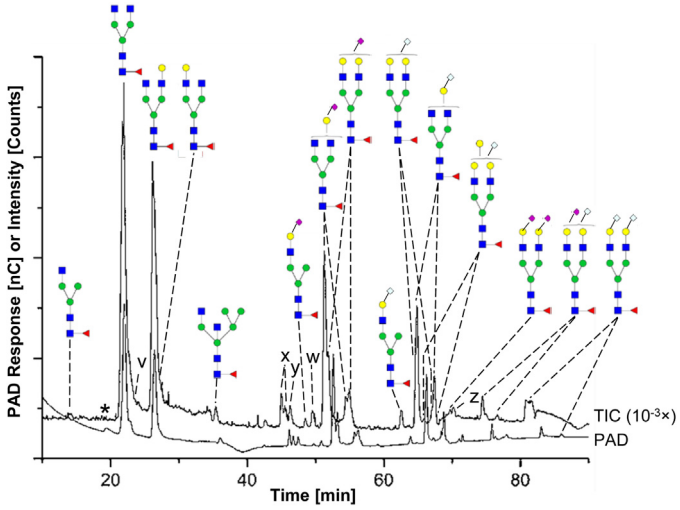

Fig. 5. HPAEC-PAD chromatograms and total ion current chromatograms from positive-mode HPAEC-MS (intensity attenuation: $10^{-3}\times$) of PNGase F-released *N*-glycans from mAb3, α2,6-sialylated with CMP-Neu5Ac. The peaks v, w, x, y and z contain glycosylamines of the *N*-glycans FA2G1NeuAc1(6), FA2G2NeuAc2(6), FA2G1NeuGc1(6) (two peaks), FA2G2NeuGc1(6) and FA2G2NeuGc2(6), respectively. *N*-glycans drawn based on the Consortium for Functional Glycomics notation. Blue square (GlcNAc), red triangle (Fuc), green circle (Man), yellow circle (Gal), pink rhomb (Neu5Ac), white rhomb (Neu5Gc). A buffer component is indicated by an asterisk.

MAb2 expressed in CHO cells has been glyco-engineered for non-fucosylation based on the overexpression of the β1,4-*N*-acetylglucosaminyltransferase III (GnT-III) and the Golgi α-mannosidase II (ManII) for increased antibody-dependent cellular cytotoxicity [32]. GnT-III transfers *N*-acetylglucosamine to the β-linked mannose in the core to generate the bisecting *N*-acetylglucosamine. The presence of this residue inhibits the action of ManII, thereby leading to an increase in especially bisected non-fucosylated and hybrid structures. The analysis of the *N*-glycans released from mAb2 revealed in total 18 different structures, the most prominent ones being complex bisected structures A2 B (35.5 min), FA2 B (34.0 min), and FA2BG1 (37.0 min) (Fig. 2B). As an example, the MS/MS spectrum of A2 B (m/z 760.9) is shown in Fig. 6B. From the parent mass m/z 760.9 ($z=2$) the composition of three hexoses and five *N*-acetylhexosamines is derived. Given that the oligosaccharide is released with PNGase F a bisected biantennary *N*-glycan is assumed. This is confirmed with MS/MS by the fragments with masses m/z 731.3 ($B_3Y_3\beta$ or D ion) and a very weak signal at m/z 510.2 (D ion − 221) [33], see Fig. 6B and Table S2 in Supplementary materials. Compared with h-IgG, mAb2 exhibit many of the same *N*-glycans (Fig. 2B), however, the distribution is changed towards the bisected structures, and complex structures like FA2 (25.0 min), FA2G1 (31.5 and 33.0 min), and FA2G2 (36.5 min) are rather low abundant. Based on integration of the single ion current chromatograms, the bisected structures account for 66% of the glycan of mAb2 and for 26% h-IgG glycans. The level of afucosylated structures of mAb2 and h-IgG sum to 41% and 10%, respectively. Also hybrid bisected structures like FM3A1 B (26.5 min), M4A1 B (30.5 min), FM5A1 B (40.0 min), and M5A1 B (41.5 min) could be verified (Fig. 2B). As expected for therapeutics expressed in CHO, the mono-sialylated FA2G1NeuAc1 and FA2G2NeuAc1 eluting at 55.0 and 56.0 min, respectively (Fig. 2B), contain α2,3-linked Neu5Ac as demonstrated by digestion with Sialidase S (data not shown).

Sp2/0 mouse myeloma cells generally produce mAbs with *N*-glycans containing α2,6-linked Neu5Gc and small amounts of α1,3-Gal. HPAEC-MS/MS of the *N*-glycans released from mAb3 revealed in total 12 different structures (Fig. 3) with the most

intense peaks representing FA2 (22.0 min) and FA2G1 (26.5 min). The MS/MS spectrum of FA2G2 with one α1,3-Gal (FA2G2Gal1) eluting at 37.0 min (Fig. 3) is shown in Fig. 6C, and further confirmed by spiking with a FA2G2Gal1 standard (data not shown). From the parent mass *m/z* 975.4 (z = 2) the composition of six hexoses, four *N*-acetylhexosamines and one deoxyhexose has been derived. Given that the oligosaccharide is released with PNGase F it represents a fucosylated biantennary *N*-glycan extended with a hexose. The glycosidic cleavage ions Y_4 (*m/z* 1584.6) and Z_4 (*m/z* 1566.5) together with the glycosidic cleavage ions *m/z* 708.4 and *m/z* 690.2 indicate that the extra hexose is situated at the non-reducing end. For more details see Fig. 6C and Table S3 in Supplementary materials. The Neu5Gc residues of all sialylated *N*-glycans could be removed by digesting with neuraminidase but not with Sialidase S (data not shown), confirming the α2,6-linkage of Neu5Gc of mAb3. Interestingly, the two isomers of the mono-sialylated, di-galactosylated *N*-glycans FA2G2NeuGc1(6) (66.4 and 68.8 min) eluted prior to the corresponding isomers of the mono-sialylated, mono-galactosylated *N*-glycans FA2G1NeuGc1(6) (66.7 and 69.1 min) (Fig. 3). This order of elution was further verified by HPAEC-MS and −PAD following a treatment with *exo*-β1,4-galactosidase releasing terminal galactose which almost completely turned the two isomer peaks of FA2G2NeuGc1(6) into two FA2G1NeuGc1(6) isomer peaks (Fig. 4). This is opposite to the order of elution of the isomers of FA2G1NeuAc1 and FA2G2NeuAc1, where the latter elutes after FA2G1NeuAc1 no matter if Neu5Ac is in the α2,3 or α2,6 position (Figs. 1, 2 and 3). As the separation by HPAEC is based on the ionizable hydroxyl groups of the monosaccharides, we speculate whether the differences in elution order of FA2G2NeuGc1(6) and FA2G2NeuAc1(6) compared to their mono-galactosylated counterparts are due to differences in the interaction of galactose hydroxyls with the ionized solid phase preventing greater interaction with the column in the case of FA2G2NeuGc1(6). As FA2G2NeuGc2(6) eluted as two peaks (> 80 min) (Fig. 3), we speculate if the latest eluting one is due to the epimerization of GlcNAc to ManNAc [34]. The two peaks eluting at 67.5 and 69.7 min were identified as mono-sialylated, di-galactosylated *N*-glycans with one α1,3-Gal (FA2G2Gal1NeuGc1(6)) by MS/MS, and the identities verified by HPAEC-MS following a digestion with α1,3-galactosidase (Fig. 4).

At 65.2 min a structure corresponding to FA1G1NeuGc1(6) eluted among the released *N*-glycans of mAb3 (Fig. 3). During biosynthesis of *N*-glycans the trimming by α-mannosidase II takes place following the transfer of an *N*-acetylglucosamine to C-2 of the mannose α1–3 in the core of $Man_5GlcNAc_2$ by *N*-acetylglucosaminyltransferase GlcNAcT-I adding an *N*-acetylglucosamine residue to the α1,3 mannose in the core of $Man_5GlcNAc_2$ [35]. We therefore assume that the peak eluting at 65.2 min corresponds to FA1G1NeuGc1(6) with Neu5Gc on the 1,3-arm of the biantennary structure. When treating with β-*N*-acetylglucosaminidase the two peaks identified as FA2G1NeuGc1(6) eluting at 66.7 and 69.1 min were almost completely absent in the PAD (Fig. 4) and TIC chromatograms (data not shown). As a consequence, the FA1G1NeuGc1(6) with Gal-Neu5Gc on the 1,3-arm eluting at 65.2 min increased in intensity as well as three other peaks containing further isobaric structures to FA1G1NeuGc1(6) eluting at 64.5, 67.7, and 68.1 min (Fig. 4). By HPAEC-MS/MS, the peak at 67.7 min proved to also include co-eluting FA2G2Gal1NeuGc1(6) as in the untreated sample. We speculate if the peak at 64.5 min represents FA1G1NeuGc1(6) with GalNeu5Gc on the 1,6-arm of the biantennary structure which is in line with the elution order of the two FA2G1 isomers. The FA1G1NeuGc1(6) eluting at 67.7, and 68.1 min could eventually be ManNAc epimers of FA1G1NeuGc1(6) with Neu5Gc on the 1,6 and 1,3 arms, respectively.

The mAb3 peaks denoted x (two peaks eluting 45.0 and 46.0 min), y (47.1 min) and z (72 min) (Fig. 3) represented *N*-glycans with masses equivalent to 1930.8 Da, 2092.8 Da, and 2400.0 Da, respectively. The MS/MS spectra allowed us to conclude that all peaks contain *N*-glycans containing one Neu5Gc. The XICs demonstrated that the y-peak was no longer detectable following digestion with *exo*-β1,4-galactosidase, whereas both x-peaks were unaffected (data not shown). Furthermore, all x, y, and z peaks disappeared when treated with neuraminidase but not with Sialidase S (data not shown), and the XICs of the peaks indicated that only the intensity of the y-peak was reduced following α2,6-sialylation with CMP-Neu5Ac (see also TIC in Fig. 5). Also the XICs confirmed that treatment with β-*N*-acetylglucosaminidase removed the two x-peaks. As the x-, y-, z-peaks exclusively disappeared following incubation at 4 °C for 1 month or treatment with 40 mM acetic acid at 45 °C for 15 min, we conclude that the peaks represent glycosylamines of FA2G1NeuGc1(6) (two peaks), FA2G2NeuGc1(6) and FA2G2NeuGc2(6), respectively. Glycosylamins have a Δmass of −1.0 Da compared to the cyclic hemiacetal of the *N*-glycans. Glycosylamines likely interact less strongly with the charged stationary phase as they possess an amino group instead of a hydroxyl group at C-1 at the reducing end, losing the most acidic hydroxylgroup [8]. Interestingly, the glycosylamines of FA2G1NeuGc1(6) and FA2G2NeuGc1(6) elute in the expected order, but opposite to the order of their corresponding cyclic hemiacetals eluting between 66.5–69.1 min (Fig. 3). The two x-peaks eluting at 45.0 and 46.0 min are likely to be the isomeric forms with Neu5Gc on the 1,6 and 1,3 arms of the biantennary structure, respectively, separated by a shallow gradient.

To increase the complexity of the *N*-glycosylation of mAb3 and to challenge the method with the separation and identification of Neu5Gc-, Neu5Ac-, and mixed Neu5Gc/Neu5Ac-containing *N*-glycans, the antibody was sialylated with Neu5Ac using the recombinant human sialyltransferase ST6Gal-I. This transferase caps penultimate galactose with sialic acids in the α2,6 position. The reaction time was set to 4 h to minimize intrinsic sialidase activity of the sialyltransferase. As a result Neu5Ac- and mixed Neu5Gc/Neu5Ac-containing *N*-glycans like FA1G1NeuAc1(6) (48.8 min), FA2G1NeuAc1(6) (51.5 and 54.5 min), FA2G2NeuAc1(6) (52.5 and 55.0 min), FA2G2NeuAc2(6) (70.0 min), and FA2G2NeuGc1NeuAc1(6) (74.5 and 77.0 min) were verified by MS/MS as separate peaks (Fig. 5). The MS/MS spectra recorded in the positive ion mode of FA2G2NeuGc1NeuAc1(6) (*m/z* 795.9 $[M+3H]^{3+}$) eluting at 74.5 min is shown in Fig. 6D. The B_3 glycosodic cleavage fragments at *m/z* 657.2 and *m/z* 673.2 show that *N*-acetylneuraminic acid and *N*-glycolylneuraminic acid is positioned in different arms of the diantennary polysaccharide and moreover is located at the non-reducing end. The very weak signals of fragments with *m/z* 981.2 ($B_5Y_3\alpha$) in combination with *m/z* 891.2 ($^{0,3}A_5Y3\alpha$) and in addition no signal was observed at *m/z* 997.3 are strongly indicative that Neu5Ac is at the non reducing end of the 1,6-arm. For more details see Table S4 in Supplementary materials. As a consequence of the sialylation with Neu5Ac, the FA2G2 (31.5 min, Fig. 5) was completely α2,6-sialylated and no more detectable by XIC evaluation. Also FA2G1 with galactose on the 1,3-arm eluting at 27.5 min (Fig. 3) was barely detectable (XIC evaluation) in the Sp2/0 material sialylated with CMP-Neu5Ac. This is consistent with the observation that the human α2,6-sialyltransferase ST6Gal-I preferentially adds sialic acid to the 1,3-arm [36,37]. HPAEC-MS and spiking with the *N*-glycan standards FA2G1NeuAc1(6), FA2G2NeuAc1(6), and FA2G2NeuAc2(6) confirmed the elution times of the Neu5Ac-containing glycan structures. The XIC chromatogram of the peak denoted v (*m/z* 958.4 (z = 2)) eluting around 23.5 min demonstrated two peaks representing the glycosylamines of FA2G1NeuAc1(6) likely to be the 1,6- and 1,3-arm forms. Similarly, the w-peak con-

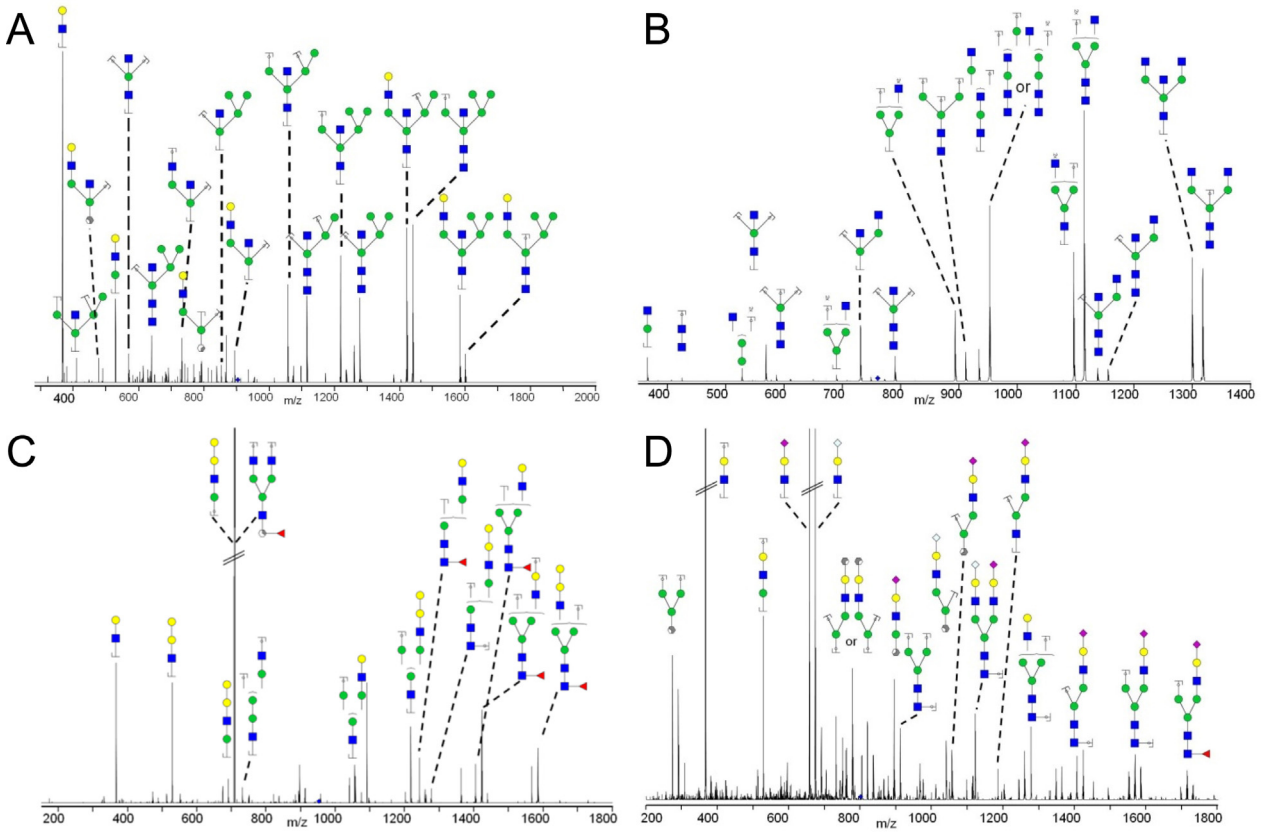

Fig. 6. MS/MS analysis of the double-protonated $[M+2H]^{2+}$ forms of (A) M5A1G1 B (*m*/*z* 902.9) of h-IgG eluting at 43.5 min (Fig. 2A), (B) A2 B (*m*/*z* 760.9) of mAb2 eluting at 35.5 min (Fig. 2B), (C) FA2G2Gal1 (*m*/*z* 975.4) of mAb3 eluting at 37.0 min (Fig. 3), and (D) triple-protonated $[M+3H]^{3+}$ FA2G2NeuGc1NeuAc1(6) (*m*/*z* 795.9) of mAb3 α2,6-sialylated with CMP-Neu5Ac eluting at 74.5 min (Fig. 5). The observed ions were interpreted according to the nomenclature of Domon and Costello [24]. Blue square (GlcNAc), red triangle (Fuc), green circle (Man), yellow circle (Gal), pink rhomb (Neu5Ac), white rhomb (Neu5Gc). Fucose re-localizations are indicated by asterisks.

tained the glycosylamine (*m*/*z* 1185.0 (z = 2)) of FA2G2NeuAc2(6). The XIC chromatogram of the mass equivalent to the glycosylamine of FA2G2NeuAc1 indicated elution shortly after the two FA2G1 peaks. Somewhat surprising, we found FA1G1NeuAc1(6) to elute at 48.8 min (Fig. 5). We speculate if this is caused by sialidase activity of the α2,6-sialyltransferase and/or due to contamination of β-*N*-acetylglucosaminidase.

3.5. *Relative quantification by specific ion current chromatograms and comparison with HPAEC-PAD and HILIC-UPLC(2-AB)*

Compared to HPAEC-PAD, HPAEC-MS has a high potential in distinguishing and allowing optimal quantification of co-eluting oligosaccharides. To test this and to compare the method with HILIC-UPLC of 2-aminobenzamide (2-AB) labelled *N*-glycans employing fluorescence detection with femtomole sensitivity [38], our preferred in-house reference method concerning robustness, accuracy, and reproducibility, a relative quantification was conducted on *N*-glycans released from CHO produced mAb4 by specific ion current (SIC) chromatogram analysis. The SIC evaluation was performed involving charge state 2+ and isotopes 0, 1 and 2. *N*-glycans were identified manually by searching their *m*/*z*-values within the experimental mass spectrum and relative amounts were calculated by integration of the SIC peaks. The HPAEC-MS data was compared to quantitative evaluations performed by HPAEC-PAD and HILIC-UPLC of 2-AB labelled *N*-glycans (Table 2). HILIC-UPLC(2-AB) was performed essentially as described by Reusch et al. [39]. Recently, we extensively characterized the *N*-glycosylation of mAb4 using in total seven non-MS methods (involving CE-LIF, HILIC, DSA-FACE, CCGE, and HPAEC [39]) and eleven MS based methods (involving MALDI-TOF, QTOF, and Orbitrap [40]). From these studies and our in-house experience we know, that the Fc-glycosylation of mAb4 involves a total of 16 detectable *N*-glycans including the two isobaric forms of both FA2G1 and A2G1. In our hands, both HPAEC-PAD (1 mm I.D. column), HPAEC-MS (1 mm I.D. column) and HILIC-UPLC(2-AB) demonstrated comparable quantitative data with low standard deviations (Table 2). With both HPAEC methods, we demonstrate the presence of all 16 distinct *N*-glycans. Using HPAEC-PAD and HPAEC-MS, the monogalactosylated structure lacking *N*-acetylglucosamine (FA1G1) was quantified to 0.4 and 0.7%, respectively. Due to co-elution with FA2G1 with β1,4-galactose on the 1,6 arm, FA1G1 was not detectable by HILIC-UPLC(2-AB) (Table 2, [39]). The levels of high mannose glycan M5 was quantified to 0.7, 0.2 and 1.5% by HPAEC-PAD, HPAEC-MS, and HILIC-UPLC(2-AB), respectively (Table 2). Column charge dependent, M5 did not elute completely base-lined separated from FA2 by HPAEC and might therefore be slightly underestimated by HPAEC-PAD. The underestimation by HPAEC-MS is likely due to ion suppression from intensive FA2 signals. Quantification by the seven different non-MS methods and the eleven MS based methods resulting in average 1.8% [39] and 1.6% M5 [40], respectively, further support the slight underestimations by both HPAEC methods. We believe further chromatographic optimization ensuring optimal separation of M5 and FA2 could eliminate this problem. Sialic acid-containing *N*-glycans are prone to fragmentation compared to neutral ones, which result in-source or metastable decay [41]. This is likely the explanation of the slightly lower levels of some of the sialylated structures of mAb4 by positive mode HPAEC-MS (Table 2).

Table 2
Quantification by integration of the HPAEC-PAD and HPAEC-MS specific ion current (SIC) chromatograms of PNGase F-released *N*-glycans from mAb4 and comparison with quantitative data from HILIC-UPLC of 2-AB labelled *N*-glycans. Relative abundances are given (bold), followed by standard deviations.

N-glycans[d]		**FA2** (G0F)	**FA2G1** (G1F)	**FA2G2** (G2F)	**FA1** (G0F-N)	**FA1G1** (G1F-N)	**A2** (G0)	**A2G1** (G1)	**A2G2** (G2)	**A1** (G0-N)	**M5**	**M6**	**FA2G1NeuAc1(3)** (G1S1F)	**FA2G2NeuAc1(3)** (G2S1F)	**FA2G2NeuAc2(3)** (G2S2F)
1 I.D. mm HPAEC-PAD[a]	AVG STD	**37.1** 0.3	**44.6** 0.4	**9.0** 0.1	**0.3** 0.0	**0.4** 0.2	**4.0** 0.2	**2.4** 0.3	**0.1** 0.0	**0.3** 0.1	**0.7** 0.3	**0.03** 0.0	**0.3** 0.2	**0.6** 0.3	**0.2** 0.1
1 I.D. mm HPAEC-MS (SIC)[a,b]		**35.4** 0.7	**46.5** 0.3	**8.8** 0.3	**0.4** 0.0	**0.7** 0.0	**3.9** 0.2	**3.0** 0.2	**0.3** 0.0	**0.3** 0.0	**0.2** 0.0	**0.1** 0.0	**0.2** 0.0	**0.2** 0.0	**0.02** 0.0
HILIC-UPLC (2-AB)[a,c]		**35.5** 0.1	**43.4** 0.1	**9.5** 0.0	**0.5** 0.0	**n.d.**	**4.6** 0.1	**3.3** 0.0	**0.3** 0.0	**0.4** 0.0	**1.5** 0.0	**0.1** 0.0	**0.2** 0.0	**0.7** 0.0	**0.1** 0.0

[a] n = 6.
[b] SIC evaluation involving charge state 2+ and isotopes 0,1 and 2.
[c] Data from Reusch et al. [39], n.d.; not detected. The *N*-glycan structures are based on the Consortium for Functional Glycomics notation.
[d] The Oxford glycan nomenclature (bold) was used for the abbreviations (alternative naming in parentheses). Blue square (GlcNAc), red triangle (Fuc), green circle (Man), yellow circle (Gal), pink rhomb (Neu5Ac).

Table 3
Quantification by integration of HPAEC-MS specific ion current (SIC) chromatograms of PNGase F-released *N*-glycans from mAb2 and comparison with quantitative data from HILIC-UPLC of 2-AB labelled *N*-glycans.

N-glycans[c]	**A2B** (G0B)	**FA2** (G0F)	**FA2B** (G0FB)	**FM3A1B** (G0F-N)	**A2G1** (G1B)	**M4A1B** (hM4B)	**FA2G1** (G1F)	**FA2G2** (G2F)	**FA2BG1** (G1FB)	**FA2BG2** (G2FB)	**A2** (G0)	**M5**	**FM5A1B** (hM5FB)	**M5A1B** (hM5B)	**M5A1BG1** (hM5G1B)	**FA2G1NeuAc1(3)** (G1S1F)	**FA2G2NeuAc1(3)** (G2S1F)
1 I.D. mm HPAEC-MS (SIC)[a,b]	**29.8**	**2.4**	**22.6**	**3.2**	**5.5**	**1.1**	**6.4**	**3.1**	**7.4**	**0.4**	**5.2**	**0.1**	**3.1**	**7.0**	**0.6**	**0.5**	**1.6**
HILIC-UPLC(2-AB)[a]	**38.9**		**28.9**		**4.6**		**3.3**	**0.6**	**8.0**	**0.3**	**6.4**	**n.q.**	**0.7**	**4.8**	**0.4**	**0.8**	**2.3**

[a] n = 1.
[b] SIC evaluation involving charge state 2+ and isotopes 0,1 and 2, n.q.; not quantifiable. The *N*-glycan structures are based on the Consortium for Functional Glycomics notation.
[c] The Oxford glycan nomenclature (bold) was used for the abbreviations (alternative naming in parentheses). Blue square (GlcNAc), red triangle (Fuc), green circle (Man), yellow circle (Gal), pink rhomb (Neu5Ac).

As relative quantification by HPAEC-MS might be even more beneficial for more heterogeneous samples of *N*-glycans, we further analyzed and quantified the *N*-glycans of mAb2 by HPAEC-MS and HILIC-UPLC(2-AB). The identification of the HILIC-UPLC(2-AB) peaks was supported by coupling with MS. By HILIC-UPLC(2-AB), A2 B and FA2 were found to co-elute, as well as FA2 B and FM3A1B, and A2G1 and M4A1B, respectively (Table 3). Furthermore, M5 eluted as a shoulder of the co-eluting FA2 B and FM3A1 B and was not quantifiable by HILIC UPLC(2-AB) (Table 3). In comparison, all mAb2 *N*-glycans could be quantified by SIC evaluation (Table 3).

4. Conclusion

Long has HPAEC been an efficient separation tool for carbohydrates and a very sensitive method in the combination with pulsed amperometric detection. Although new mass spectrometry based and high-resolving separation based methods like porous graphitized carbon, reverse phase and hydrophilic interaction liquid chromatography of unlabeled or labelled *N*-glycans have evolved, HPAEC coupled with MS with its selectivity towards carbohydrate charge, composition, size and linkage positions of oligosaccharides is a competitive technique in the characterization of complex samples. A major benefit of HPAEC is still that it does not require

derivatization or any clean-up procedures of the released *N*-glycans to quantitate and characterize even low abundant glycan species. The biggest challenge in coupling HPAEC with MS is, however, to remove the high concentrations of salts from the mobile phases prior to detection by MS, which is done by using a suppressor that exchanges Na^+ ions with H^+ ions.

Here we tested the coupling of mini-bore HPAEC with MS for the structural assignment and quantification of heterogeneous sources of IgG derived *N*-glycans. With the mini-bore column we obtained a significant limit of detection improvement of 2–8 folds for *N*-glycan standards compared with an analytical scale 3 mm column. We could demonstrate femtomole sensitivities for both PAD and MS detection using the 1 mm column. HPAEC-MS/MS allowed the assignment of a significant number of major and minor peaks to *N*-glycan structures including complex-type, high mannose, hybrid and hybrid bisected structures. We conclude that the coupling of mini-bore HPAEC to MS demonstrated a superior performance with respect to selectivity in the relative quantification of complex mixtures of *N*-glycans. With the gain in sensitivity compared to analytical scale mid-size (3 mm I.D.) HPAEC, the mini-bore HPAEC-MS/MS method is an attractive and stable method in the biomedical research and for the characterization of e.g. IgG biopharmaceuticals, especially when the glycosylation pattern is more heterogeneous like in the case of glyco-engineered mAbs.

Acknowledgements

Dr. Markus Roessler and Dr. Stefan Fiedler (Roche Diagnostics GmbH, Penzberg, Germany) are thanked for providing the purified h-IgG. Cees Bruggink and Manfred Wuhrer acknowledge support by the European Union (Seventh Framework Programme HighGlycan project, grant number 278535).

Appendix A. Supplementary data

Supplementary data associated with this article can be found, in the online version, at http://dx.doi.org/10.1016/j.jchromb.2016.08.001.

References

[1] D. Reusch, M.L. Tejada, Fc glycans of therapeutic antibodies as critical quality attributes, Glycobiology 25 (2015) 1325–1334.
[2] V. Dotz, R. Haselberg, A. Shubhakar, R.P. Kozak, D.F. Yoann Rombouts, D. Reusch, G.W. Somsen, D.L. Fernandes, M. Wuhrer, Mass spectrometry for glycosylation analysis of biopharmaceuticals, Trends Anal. Chem. 73 (2015) 1–9.
[3] M.R. Hardy, R.R. Townsend, Separation of positional isomers of oligosaccharides and glycopeptides by high-performance anion-exchange chromatography with pulsed amperometric detection, Proc. Natl. Acad. Sci. U. S. A. 85 (1988) 3289–3293.
[4] R.R. Townsend, M.R. Hardy, O. Hindsgaul, Y.C. Lee, High-performance anion-exchange chromatography of oligosaccharides using pellicular resins and pulsed amperometric detection, Anal. Biochem. 174 (1988) 459–470.
[5] R.R. Townsend, M.R. Hardy, D.A. Cumming, J.P. Carver, B. Bendiak, Separation of branched sialylated oligosaccharides using high-pH anion-exchange chromatography with pulsed amperometric detection, Anal. Biochem. 182 (1989) 1–8.
[6] J.L. Behan, K.D. Smith, The analysis of glycosylation: a continued need for high pH anion exchange chromatography, Biomed. Chromatogr. 25 (2011) 39–46.
[7] T.R. Cataldi, C. Campa, G.E. De Benedetto, Carbohydrate analysis by high-performance anion-exchange chromatography with pulsed amperometric detection: the potential is still growing, Fresenius, J. Anal. Chem. 368 (2000) 739–758.
[8] Y.C. Lee, High-performance anion-exchange chromatography for carbohydrate analysis, Anal. Biochem. 189 (1990) 151–162.
[9] M.W. Spellman, Carbohydrate characterization of recombinant glycoproteins of pharmaceutical interest, Anal. Chem. 62 (1990) 1714–1722.
[10] K.D. Smith, E.F. Hounsell, J.M. McGuire, M.A. Elliott, H.G. Elliott, Structural elucidation of the N-linked oligosaccharides of glycoproteins using high pH anion-exchange chromatography, in: R.J. Sturgeon (Ed.), Advances in Macromolecular Carbohydrate Research, Elsevier, Amsterdam, 1997.
[11] J.S. Rohrer, Separation of asparagine-linked oligosaccharides by high-pH anion-exchange chromatography with pulsed amperometric detection: empirical relationships between oligosaccharide structure and chromatographic retention, Glycobiology 5 (1995) 359–360.
[12] J.J. Conboy, J. Henion, High-performance anion-exchange chromatography coupled with mass spectrometry for the determination of carbohydrates, Biol. Mass Spectrom. 21 (1992) 397–407.
[13] R.A.M. van der Hoeven, W.M.A. Niessen, H.A. Schols, C. Bruggink, A.G.J. Voragen, J. van der Greef, Characterization of sugar oligomers by on-line high-performance anion-exchange chromatography-thermospray mass spectrometry, J. Chromatogr. A 627 (1992) 63–73.
[14] S. Richardson, A. Cohen, L. Gorton, High-performance anion-exchange chromatography-electrospray mass spectrometry for investigation of the substituent distribution in hydroxypropylated potato amylopectin starch, J. Chromatogr. A. 917 (2001) 111–121.
[15] C. Bruggink, R. Maurer, H. Herrmann, S. Cavalli, F. Hoefler, Analysis of carbohydrates by anion exchange chromatography and mass spectrometry, J. Chromatogr. A 1085 (2005) 104–109.
[16] C. Bruggink, M. Wuhrer, C.A. Koeleman, V. Barreto, Y. Liu, C. Pohl, A. Ingendoh, C.H. Hokke, A.M. Deelder, Oligosaccharide analysis by capillary-scale high-pH anion-exchange chromatography with on-line ion-trap mass spectrometry, J. Chromatogr. B (2005) 136–143.
[17] C. Bruggink, B.J. Poorthuis, A.M. Deelder, M. Wuhrer, Analysis of urinary oligosaccharides in lysosomal storage disorders by capillary high-performance anion-exchange chromatography-mass spectrometry, Anal. Bioanal. Chem. 403 (2012) 1671–1683.
[18] G. Chataigné, F. Couderc, V. Poinsot, Polysaccharides analysis of sinorhizobial capside by on-line anion exchange chromatography with pulsed amperometric detection and mass spectrometry coupling, J. Chromatogr. A 1185 (2008) 241–250.
[19] H.A. Schols, M. Mutter, A.G. Voragen, W.M. Niessen, R.A. van der Hoeven, J. van der Greef, C. Bruggink, The use of combined high-performance anion-exchange chromatography-thermospray mass spectrometry in the structural analysis of pectic oligosaccharides, Carbohydr. Res. 261 (1994) 335–342.
[20] S. Wouters, B. Wouters, S. Jespers, G. Desmet, H. Eghbali, C. Bruggink, S. Eeltink, Design and performance evaluation of a microfluidic ion-suppression module for anion-exchange chromatography, J. Chromatogr. A 1355 (2014) 253–260.
[21] J.R. Thayer, J.S. Rohrer, N. Avdalovic, R.P. Gearing, Improvements to in-line desalting of oligosaccharides separated by high-pH anion exchange chromatography with pulsed amperometric detection, Anal. Biochem. 256 (1998) 207–216.
[22] D. Damerell, A. Ceroni, K. Maass, R. Ranzinger, A. Dell, S.M. Haslam, The GlycanBuilder and GlycoWorkbench glycoinformatics tools: updates and new developments, Biol. Chem. 393 (2012) 1357–1362.
[23] C. Guignard, L. Jouve, M.B. Bogéat-Triboulot, E. Dreyer, J.F. Hausman, L. Hoffmann, Analysis of carbohydrates in plants by high-performance anion-exchange chromatography coupled with electrospray mass spectrometry, J. Chromatogr. A 1085 (2005) 137.
[24] B. Domon, C.E. Costello, A systematic nomenclature for carbohydrate fragmentations in FAB-MS/MS spectra of glycoconjugates, Glycoconj. J. 5 (1988) 397–409.
[25] M. Wuhrer, A.M. Deelder, Y.E. van der Burgt, Mass spectrometric glycan rearrangements, Mass Spectrom. Rev. 30 (2011) 664–680.
[26] D.J. Harvey, Fragmentation of negative ions from carbohydrates: part 1. Use of nitrate and other anionic adducts for the production of negative ion electrospray spectra from N-linked carbohydrates, J. Am. Soc. Mass Spectrom. 16 (2005) 622–630.
[27] R. Gill, B. Law, Appraisal of narrow-bore (1 mm I.D.) high-performance liquid chromatography columns with view to the requirements of routine drug analysis, J. Chromatogr. 354 (1986) 185–202.
[28] C. Grey, P. Edebrink, M. Krook, S.P. Jacobsson, Development of a high performance anion exchange chromatography analysis for mapping of oligosaccharides, J. Chromatogr. B 877 (2009) 1827–1832.
[29] D.J. Harvey, Postsource decay fragmentation of N-linked carbohydrates from ovalbumin and related glycoproteins, J. Am. Soc. Mass Spectrom. 11 (2000) 572–577.
[30] R. Jassal, N. Jenkins, J. Charlwood, P. Camilleri, R. Jefferis, J. Lund, Sialylation of human IgG-Fc carbohydrate by transfected rat alpha2,6-sialyltransferase, Biochem, Biophys. Res. Commun. 286 (2001) 243–249.
[31] R.M. Anthony, F. Nimmerjahn, D.J. Ashline, V.N. Reinhold, J.C. Paulson, J.V. Ravetch, Recapitulation of IVIG anti-inflammatory activity with a recombinant IgG Fc, Science 320 (2008) 373–376.
[32] C. Ferrara, P. Brünker, T. Suter, S. Moser, U. Püntener, P. Umaña, Modulation of therapeutic antibody effector functions by glycosylation engineering: influence of Golgi enzyme localization domain and co-expression of heterologous beta1,4-N-acetylglucosaminyltransferase III and Golgi α-mannosidase II, Biotechnol. Bioeng. 93 (2006) 851–861.
[33] D.J. Harvey, Fragmentation of N-linked glycans with a matrix-assisted laser desorption/ionization ion trap time-of-flight mass spectrometer, Rapid Commun. Mass Spectrom. 18 (2004) 2997–3007.
[34] T. Toida, I.R. Vlahov, A.E. Smith, R.E. Hileman, R.J. Linhardt, C-2 epimerization of N-acetylglucosamine in an ligosaccharide derived from heparan sulfate, J. Carbohydr. Chem. 15 (1996) 351–360.

[35] P. Hossler, S.F. Khattak, Z.J. Li, Optimal and consistent protein glycosylation in mammalian cell culture, Glycobiology 19 (2009) 936–949.
[36] A.W. Barb, E.K. Brady, J.H. Prestegard, Branch-specific sialylation of IgG-Fc glycans by ST6Gal-I, Biochemistry 48 (2009) 9705–9707.
[37] M. Thomann, T. Schlothauer, T. Dashivets, S. Malik, C. Avenal, P. Bulau, P. Rüger, D. Reusch, In vitro glycoengineering of IgG1 and its effect on Fc receptor binding and ADCC activity, PLoS One 10 (2015) e0134949, http://dx.doi.org/10.1371/journal.pone.0134949, eCollection 2015.
[38] P.M. Rudd, R.A. Dwek, Rapid, sensitive sequencing of oligosaccharides from glycoproteins, Curr. Opin. Biotechnol. 8 (1997) 488–497.
[39] D. Reusch, M. Haberger, B. Maier, M. Maier, R. Kloseck, B. Zimmermann, M. Hook, Z. Szabo, S. Tep, J. Wegstein, N. Alt, P. Bulau, M. Wuhrer, Comparison of methods for the analysis of therapeutic immunoglobulin G Fc-glycosylation profiles-Part 1: separation-based methods, MAbs 7 (2015) 167–179.
[40] D. Reusch, M. Haberger, D. Falck, B. Peter, B. Maier, J. Gassner, M. Hook, K. Wagner, L. Bonnington, P. Bulau, M. Wuhrer, Comparison of methods for the analysis of therapeutic immunoglobulin G Fc-glycosylation profiles-Part 2: mass spectrometric methods, MAbs 7 (2015) 732–742.
[41] K.R. Reiding, D. Blank, D.M. Kuijper, A.M. Deelder, M. Wuhrer, High-throughput profiling of protein N-glycosylation by MALDI-TOF-MS employing linkage-specific sialic acid esterification, Anal. Chem. 86 (2014) 5784–5793.